# EXPLORE WHAT'S NEW IN
THE RIT FAMILY OF PRODUCTS VERSION 6.11
MEDICAL PHYSICS' MOST ADVANCED QA SOFTWARE

### Varian Halcyon® RapidArc® & Picket Fence Analysis

By popular demand, RIT has extended our traditional RapidArc MLC analyses to support Varian Halcyon LINACs. In addition to the Millennium 120 and HD120 models, Halcyon users now have the option to perform fully automated RapidArc QA, with the flexibility to use distal, proximal, or dual MLC configurations.
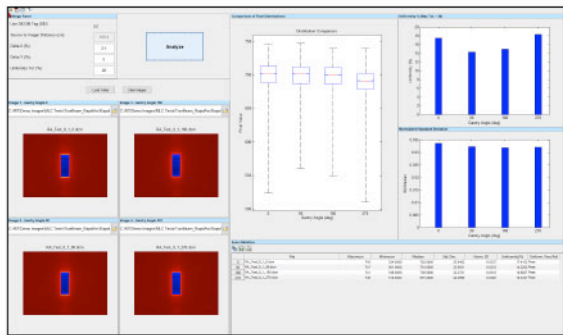
New Routines & Workflow for Varian RapidArc® Tests

The new RapidArc Test 0.1 (dMLC Dosimetry) interface simultaneously loads and analyzes four cardinal gantry angle images and provides full automation for quick results. The software also features the new RapidArc Test 2 (Dose Rate and Gantry Speed) and Test 3 (Leaf Speed) routines for analyzing the various test modes against an open field image.

Enhanced MLC QA Automation Workflow
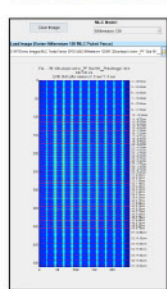
RapidArc Tests 0.2, 1.1, and 1.2, and the standard Picket Fence tests have been enhanced with (1) automated pre-processing for rotational and translation alignment, (2) expanded individual leaf analysis, and (3) support for a variety of common EPID sizes: 30x30, 30x40, 40x30, 40x40, and 43x43 cm.

### Plan-Based Calibration for TomoTherapy® Registration

Utilize RIT's patented PBC technology to simplify your TomoTherapy Registration process for patient QA. A calibration file is no longer needed, scanner warm up is minimized, and variation in development time after exposure is no longer a significant factor. This saves you time and money, and potentially improves patient throughput.

Enhanced & Expanded Isocenter Optimization

RIT's popular 3D Winston-Lutz (Isocenter Optimization) routine now supports analysis on Elekta Unity machines. The updated interface will also display a range of 3 to 16 images within the same interface window. File names for exported results are automatically generated, saving users time. Choose to pass or fail on the Maximum Machine Deviation (R) or the Total Maximum Deviation (W), which includes the ball setup error.

EPID QA Phantom Couch Analysis

RIT software will analyze the EPID QA phantom when placed directly on the couch, providing an analysis closer to realistic patient positioning. The phantom's magnified dimensions are automatically calculated from the phantom size. This update provides physicists with more setup options when performing phantom analyses.
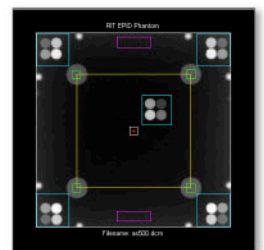
Expanded Phantom Analyses

RIT's Catphan Materials analysis will now analyze both horizontal slices and both vertical slices with ramps, in addition to an added measure of the yaw and tilt of the phantom, based on these ramps. Analyses for the QC-3 and QC-kV1 phantoms now feature a uniformity analysis.
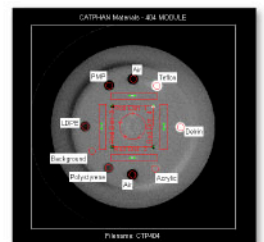
CLICK TO EXPLORE THE NEW FEATURES IN DETAIL

RESEARCH ARTICLE

Rapid estimation of patient-specific organ doses using a deep learning network

Marios Myronakis[1] | **John Stratakis**[1,2] | **John Damilakis**[1,2]

[1]Department of Medical Physics, School of Medicine, University of Crete, Iraklion, Greece

[2]Medical Physics Department, University Hospital of Crete, Iraklion, Greece

Correspondence
Marios Myronakis
Email: mmyronakis@bwh.harvard.edu

Funding information
Euratom research and training programme 2019–2020, Grant/Award Number: 945196

Abstract

Background: Patient-specific organ-dose estimation in diagnostic CT examinations can provide useful insights on individualized secondary cancer risks, protocol optimization, and patient management. Current dose estimation techniques mainly rely on time-consuming Monte Carlo methods or/and generalized anthropomorphic phantoms.

Purpose: We proposed a proof-of-concept rapid workflow based on deep learning networks to estimate organ doses for individuals following thorax Computed Tomography (CT) examinations.

Methods: CT scan data from 95 individuals undergoing thorax CT examinations were used. Monte Carlo simulations were performed and three-dimensional (3D) dose distributions for each patient were obtained. A fully connected sequential deep learning network model was constructed and trained for each organ considered in this study. Water-equivalent diameter (WED), scan length, and tube current were the independent variables. Organ doses for heart, lungs, esophagus, and bones were calculated from the Monte Carlo 3D distribution and used to train the deep learning networks. Organ dose predictions from each network were evaluated using an independent data set of 19 patients.

Results: The trained networks provided organ dose predictions within a second. There was very good agreement between the deep learning network predictions and reference organ dose values calculated from Monte Carlo simulations. The average difference was −1.5% for heart, −1.6% for esophagus, −1.0% for lungs, and −0.4% for bones in the 95 patients dataset, and −5.1%, 4.3%, 0.9%, and 1.4% respectively in the 19 patients test dataset.

Conclusions: The proposed workflow demonstrated that patient-specific organ-doses can be estimated in nearly real-time using deep learning networks. The workflow can be readily implemented and requires a small set of representative data for training.

KEYWORDS
CT, deep learning, dosimetry

1 | INTRODUCTION

Patient dose estimation during diagnostic CT examinations has been a matter of research, scrutiny, and legislation since the adoption of CT as the workhorse of radiological departments.[1–3] Traditional methods to estimate patient dose, rely on standardized phantom-based measurements using TLDs or other detectors to provide either point estimates or 2D distributions of dose. Although these methods clearly depict dose distributions from actual measurements, they fall short on doing so on real patients rather than phantoms. In the past decade, Monte Carlo based dose estimation techniques have increasingly been applied as more computing power became available.[4–7] However, Monte Carlo computations are often time-consuming, laborious
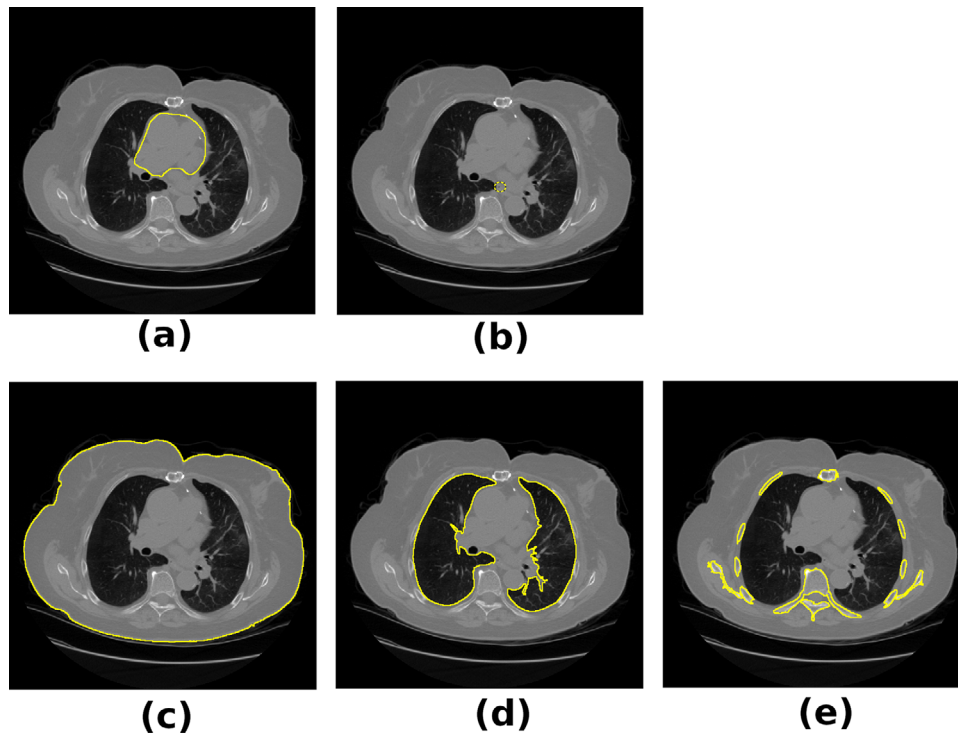
FIGURE 1 Manually delineated organs, (a) heart, (b) esophagus, and automatically delineated organs using thresholding techniques, (c) body, (d) lungs, (d) bone structure. (W: 1550, L: −250).

to properly setup, and often need specific knowledge of the Monte Carlo software at hand. This can be challenging to clinics, especially to those with high patient throughput, where a rapid workflow is required. In addition, Monte Carlo based computations rely solely on a computerized representation of the scanner characteristics and the patient, usually through a set of CT images, which increases the potential uncertainty on the final dosimetric outcome.

With the advent of artificial intelligence in medical applications, solutions that provided accurate dose estimations based on deep learning algorithms emerged[8–10] mainly at the radiotherapy field. These solutions rely on image generation using generalized adversarial networks (GAN) or other types of convolutional neural networks. The training difficulty and the need for successive deep learning algorithms for various steps of the dose estimation procedure (e.g., image generation, segmentation, final estimation of absolute dose) may provide additional challenges in implementation and daily use within the workflow of a clinic. These methods employ deep learning network training based on a predetermined set of dose distributions, estimated through Monte Carlo or analytical approximations of dose deposition. The deep learning network is trained to generate dose images within the range of the predetermined dose distributions. In a subsequent step, another deep learning model can be implemented and trained to automate organ segmentation.

There is a potential exploitation of the initial dose distribution obtained through Monte Carlo, to create a shortcut to the organ dose estimation procedure. Instead of using the 3D dose distributions as training material for the deep learning networks, one can first calculate organ doses and then train a network to directly provide organ dose values rather than images. Furthermore, instead of using a CT image as input, specific parameters included in or derived from the CT images can be associated with patient-specific organ doses and used as independent variables. This modification can bypass the difficulties and steps required with image generation through image-generating deep learning networks. The aim of the current work was to propose a proof-of-concept for a rapid workflow based on a deep learning neural network to estimate patient-specific organ doses from thorax CT examinations without the need for dose image generation or/and segmentation.

2 | METHODS

2.1 | Patient CT data collection

Volumetric image data from 95 adult individuals undergoing thorax CT examinations with GE Revolution GSI 64 were collected. The average age was 64.3 years (SD: ±16 years) and the median age was 67 years. Truncated volumes or studies acquired using contrast-enhancement were not considered to avoid biasing the dosimetric estimation due to missing tissue data and increased x-ray transmission/absorption respectively.
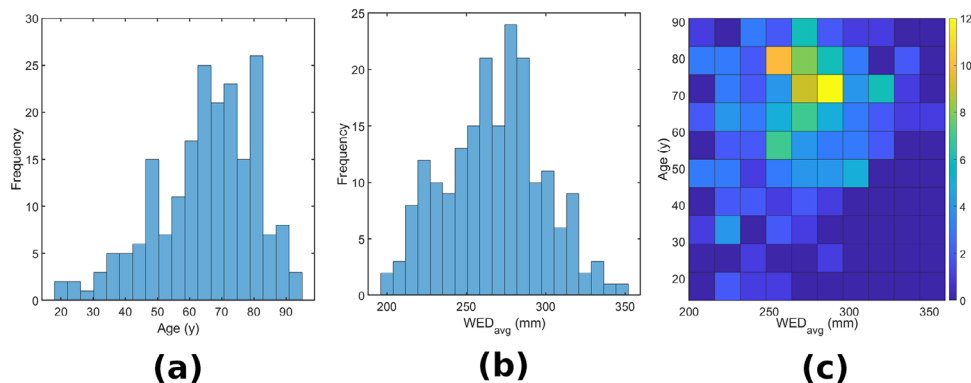
FIGURE 2 (a) Age distribution among the patients selected in this work. (b) Distribution of WED_{avg} in the thoracic region. (c) 2D histogram of WED_{avg} versus patient age.

Another dataset of 19 patients with similar characteristics and exclusion criteria were collected for algorithm testing. This dataset was not used during training and validation. The study was retrospective and patient consent was not required. An Institutional Review Board approval to process anonymized images was granted.

Patient CT scans were performed with predefined protocols suitable for thoracic imaging in all scanners. In a standard thoracic protocol, the scanned anatomy is defined as just before the apices to just above adrenals. These protocols have specific settings that were translated to corresponding parameter values in ImpactMC Monte Carlo software. The number of rotations per simulation was calculated based on the length of the imaged volume, beam collimation, and pitch.

2.2 | Body and organ delineation

The Fiji image processing package[11] was utilized to delineate radiosensitive organs within the primary exposed volume. Esophagus, and heart were manually delineated by an experienced operator. Bone structure and lungs were automatically delineated using the iso-data clustering algorithm of Ridler & Calvard.[12] The algorithm segments the image into object and background using an initial threshold, and then iteratively updates the segmentation threshold based on border pixel averaging. Automatically delineated organs were reviewed by the same radiologist for adjustments and modifications.

2.3 | Wed calculation

Water equivalent diameter (WED) is a patient size metric that accounts for patient attenuation characteristics and can be derived from CT images. The WED calculation method is thoroughly described in AAPM Report 220.[13] The following equation was applied at each CT slice in every patient CT scan included in this study:

$$\text{WED} = 2 \times \sqrt{\left[\frac{1}{1000}\overline{HU}_{body} + 1\right] \times \frac{A_{body}}{\pi}} \qquad (1)$$

where $\overline{HU}_{body}$ is the average CT-value along the outline of the patient at a specific CT slice and A_{body} is the area of the body outline.

2.4 | Monte Carlo software for dose estimation

The Monte Carlo software selected for dosimetric computations was ImpactMC (version 1.6, CT Imaging GMBH, Erlangen, Germany).[5] ImpactMC is a well-validated Monte Carlo software, specifically designed for 3D dosimetric evaluation on CT-acquired images.[5,14,15] Dose is calculated on a per image voxel basis, considering all available physical interactions for photons up to 200 keV and local deposition for electrons. ImpactMC utilizes any available graphics processing unit (GPU) to accelerate computations.

Dose estimation through ImpactMC requires an input volume, that is, a set of CT reconstructed images from one examination in DICOM format. In the current work the input volume is individual thoracic CT from scans collected as described in II.A. In addition, the software requires scanner parameters, that is, the beam spectrum, filtration, and geometrical specifications (described in subsequent paragraphs). Finally, simulation parameters, for example, the number of simulated x-rays and sampling angles per rotation need to be defined. Good statistical performance (<1% uncertainty) was obtained using a value in the order of 10^9 interacting x-rays. The time required to perform a helical CT simulation with pitch equal to one and rotation time equal to 1 s using an input CT image set with 150 slices and 10^9 x-rays was approximately 180 s in a GTX 1660 GPU.
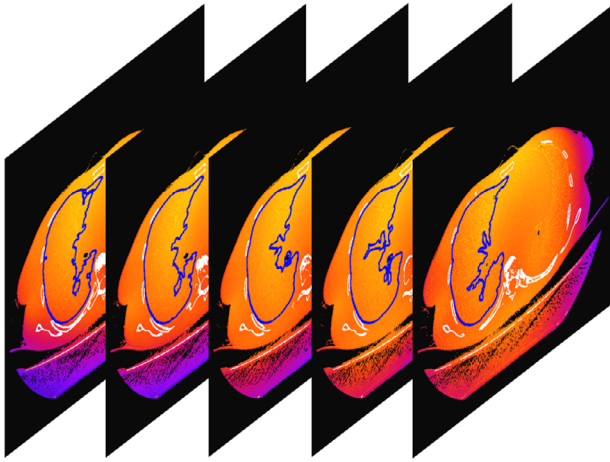
FIGURE 3 Right lung contours overlaid on corresponding dose slices for organ-dose calculation.

2.5 | Scanner parameters

Scanner-specific dose estimation required the parameterization of the Monte Carlo software according to operating and physical characteristics of each scanner considered. The CT scanner model were based on data for x-ray beam spectra, beam shaping devices (bowtie filters), and geometrical specifications. The required data were provided by the manufacturer and later compiled and converted to input parameters suitable for the Monte Carlo software. The CT scanner modeled was the GE Revolution GSI 64. The focus to isocenter distance was 539 mm with a fan angle of 56 degrees. The beam can be collimated up to 40 mm and there are three beam-shaping devices (small, medium, large) that can be used based on the field-of-view.

The scanner modeled in the current work was capable for fixed and modulated current acquisitions. Simulation of transient current modulation (TCM) was based on mA values stored in the 'x-ray Tube Current' DICOM tag (0018, 1151). These mA values represent the average of angularly and longitudinally modulated current applied along gantry rotation during image acquisition. TCM was obtained from DICOM header information within each image. The TCM value from each image was extracted and imported in the Monte Carlo software. Dose distributions for every patient in this study were generated using individual TCM.

The CT scan of each patient was used as input volume to perform dosimetric computations at 120 kV. Separate computations were performed for modulated and fixed current. The average tube current value was set equal to 100 mA over 1 s gantry rotation. Tube current normalization to 100 mA simplifies dose output processing without loss of accuracy. The shape of the current modulation is preserved, the 100 mA is just scaling that does not affect in any way the modulation. For

organ dose calculations, the current is scaled back to the original values.

The Monte Carlo software output after each computation was in the form of three-dimensional (3D) dose distribution. Each slice of the distribution corresponds to the same slice in the CT scan. Each pixel in a specific slice of the CT volume has a corresponding dose value in the 3D dose distribution output. The dose distribution was exported in binary format with 32-bit floating point precision. To facilitate dose data processing, the output dose was normalized to CT dose index in free air ($CTDI_{air}$). CTDIair normalized to 100 mAs depends on beam energy and collimation hence the operation is easily reversable to retrieve the absolute dose. The unit of dose values in the 3D volume was mGy/mGy per 100 mAs.

Organ-dose information was extracted from 3D dose distributions through appropriate delineation described in §II.B. The organs of interest in this work were bones, lungs, esophagus, and heart. The contours of each organ were overlaid on the corresponding slices of the dose distribution and the respective dose was extracted. The dose over the whole organ was computed as:

$$D = \sum_i^N D_i \qquad (2)$$

where, D_i is the dose within the contour at slice i, and N the total number of slices that contain contours of a specific organ. The calculated organ-dose (D) was normalized to 100 mA, pitch factor (p) equal to one, and rotation time (t_{rot}) equal to 1 s using the following formula:

$$D_n = D \times \frac{p \times 100}{t_{rot} \times mA} \qquad (3)$$

where D_n is the normalized organ-dose in mGy/mGy per 100 mAs.

2.6 | Deep learning network architecture and training

The deep learning network architecture was implemented in MATLAB using the Deep Learning Toolbox.[16] The network was composed of three fully connected hidden layers with rectified linear activation functions (ReLU). The number of nodes in each hidden layer was 200, 100, and 50 respectively. The final layer was a regression layer.

The independent variables were the scan length, the average current value (mA_{avg}), and the average WED value for each patient. Scan length and mA_{avg} can be readily calculated from the DICOM header of the CT images. WED_{avg} was calculated as the average of all

WED values along one patient, for each patient in the dataset. The dependent variable was total dose per organ, estimated through Monte Carlo simulations for each patient. A network was trained separately for each organ included in this work, namely, lungs, bone, heart, and esophagus. The networks with best performance were selected after applying 10-fold cross-validation to the dataset. The metrics used to determine training convergence and performance was accuracy (defined as 1-validation loss). The networks were trained for 500 epochs. Training and validation datasets were drawn from the 95 patients dataset. During the 10-fold cross-validation, the dataset was split to 90% and 10% training and validation respectively. Independent testing of the algorithm was performed on the 19 patients dataset that was not used for training nor validation.

The estimated organ dose produced using the deep learning network (D_{organ}^{DL}) was compared to the organ dose obtained using Monte Carlo estimation (D_{organ}^{MC}) using the percent relative difference ($R_{organ}\%$) as:

$$R_{organ}\% = \frac{\left(D_{organ}^{DL} - D_{organ}^{MC}\right)}{D_{organ}^{MC}} \times 100 \qquad (4)$$

3 | RESULTS

Manual delineation of various organs and tissues for a female patient is demonstrated in Figure 1a,b. Automatic delineation of body, lungs, and bones for the same patient is depicted in Figure 1c-e.

Average WED values were calculated along the scanned thorax region for each patient. The maximum WED_{avg} was equal to 351 mm and the minimum was 201 mm. The mean WED_{avg} value was 267 mm (SD:±31 mm) and the median was 271 mm. WED_{avg} distributions and corresponding patient age are depicted in Figure 2b,a respectively. The selected patient population has a wide range of WED_{avg} values despite the slightly skewed distribution of patient age toward elderly patients. Figure 2c depicts a two-dimensional correlation between WED_{avg} versus patient age.

Monte Carlo based dose distributions corresponding to CT images of all patients in this study were generated and organ-doses were estimated as described in §II.F (Figure 3). The validation accuracy of the trained networks for each organ was 1 (down to the 3rd decimal).

In Table 1, the average relative difference between Monte Carlo estimated and deep learning network generated organ dose values is demonstrated along with the associated error range for the 95 patients training dataset. In Figures 4–7, organ dose estimated values generated using the deep learning algorithm for the respective dataset were compared with Monte Carlo

TABLE 1 Average error and standard deviation between deep learning network and Monte Carlo estimated organ-dose values in the training dataset

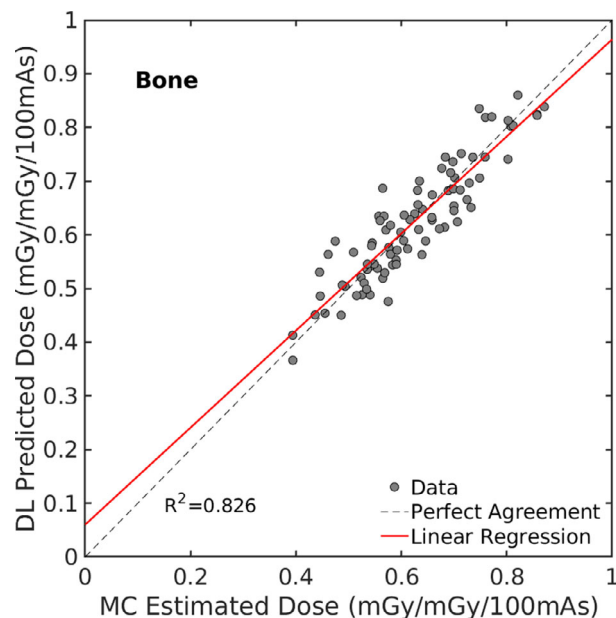| Organ	Average relative error	Standard deviation
Bones	−0.4%	8.0%
Esophagus	−1.6%	6.9%
Heart	−1.5%	7.6%
Lungs	−1.0%	10.5%

FIGURE 4 Plot of deep learning predicted dose against Monte Carlo estimated dose for bone tissue (training dataset). Linear regression is shown with red line ($R^2 = 0.826$). Perfect agreement is depicted with dashed line.
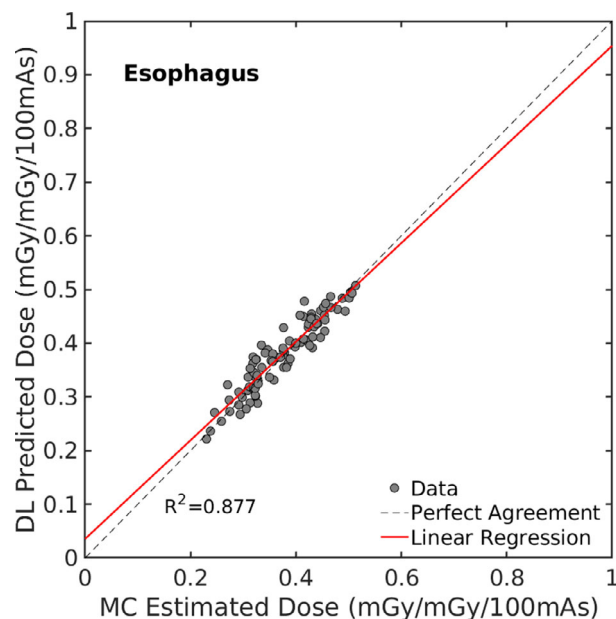

FIGURE 5 Plot of deep learning predicted dose against Monte Carlo estimated dose for esophagus tissue (training dataset). Linear regression is shown with red line ($R^2 = 0.877$). Perfect agreement is depicted with dashed line.
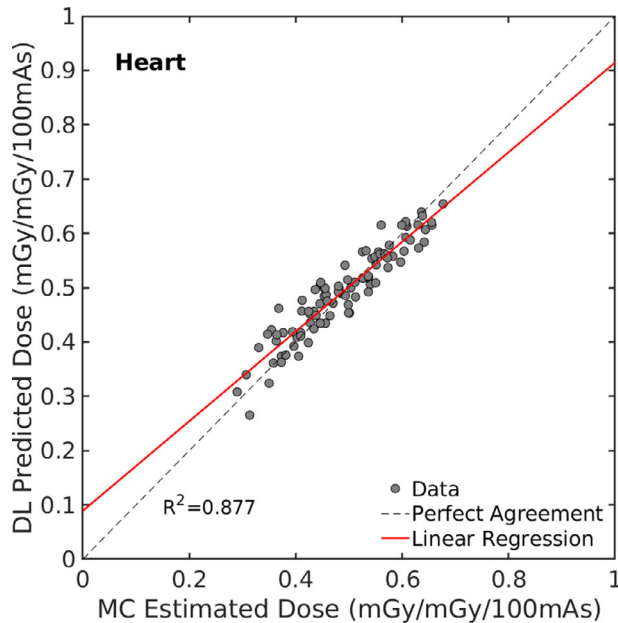
FIGURE 6 Plot of deep learning predicted dose against Monte Carlo estimated dose for heart tissue (training dataset). Linear regression is shown with red line ($R^2 = 0.877$). Perfect agreement is depicted with dashed line.
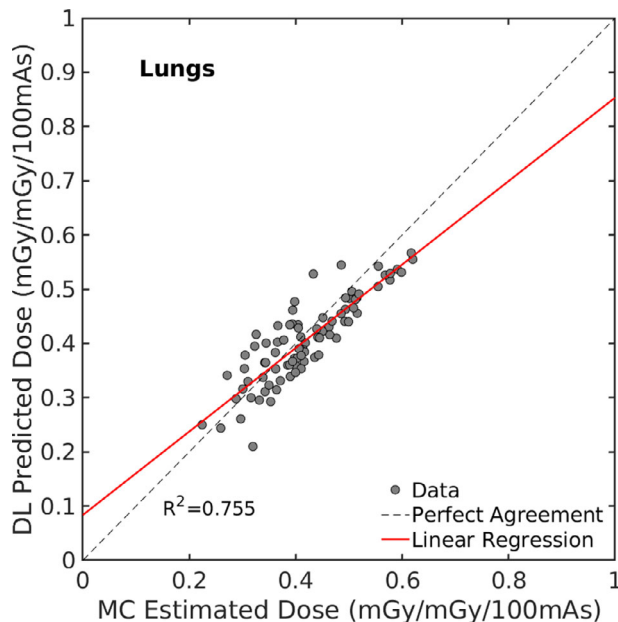

FIGURE 7 Plot of deep learning predicted dose against Monte Carlo estimated dose for lung tissue (training dataset). Linear regression is shown with red line ($R^2 = 0.755$). Perfect agreement is depicted with dashed line.

based organ dose values for each organ considered in this work, namely bones, esophagus, lung, and heart. The time required to generate predictions with the deep learning network was less than a second.

The relative prediction error between deep learning predicted and Monte Carlo estimated organ-dose values in the independent test dataset of 19 patients is demon-strated in Figures 8–11. In all test cases the largest error was below 25%.

4 | DISCUSSION

In this work we demonstrated a proof-of-concept methodology for rapid prediction of patient-specific organ doses from thoracic CT examinations using deep learning algorithms and a limited set of training data. The method relied on precalculated organ doses using Monte Carlo generated dose distributions of over 95 patients to establish the training and validation sets. A deep learning network was trained to produce patient-specific organ dose estimates using WED, scan length, and average mAs of each patient as the independent variables.

The purpose of this study was to suggest a deep-learning network model that generates organ-dose images without the need for large training datasets and dose distribution image generation. The method demon-strated a particular example for a thoracic protocol for specific vendor. Since the doses are normalized the training model can be easily applied to the same CT model at different clinics. We have not tested the appli-cation of the model for scanner from different vendors and other protocols. It is likely that in those cases, a new training set will be needed to train the model. A potential challenge is the need for vendor-specific data to model the CT scanner for the Monte Carlo dose estimation step required for training the deep learning algorithm. It is unlikely that characteristics such as x-ray spectra, and bow-tie filter shape and materials are publicly available for every possible scanner. However, this is a challenge for any other deep learning algorithm (or Monte Carlo software) that aims to estimate patient-specific dose. On-site determination of CT scanner characteristics using appropriate measurement techniques may pro-vide a good alternative, when vendor-specific data are not readily available.

There was good agreement between the deep learn-ing algorithm and Monte Carlo organ dose estimates in the training and the test dataset. The relative difference in any organ was on average within 2% in the training dataset and 5% in the test dataset; in two cases only, this difference reached 24.7%. The observed differences are considered acceptable for dosimetry in diagnostic CT. It is not uncommon to observe uncertainties up to 20% in CT figures of merit such as CTDI; manufacturers cite uncertainties up to 30% over several measurements with the same CT model as a result of variations in tube output.[*] Although there were only three indepen-dent variables used to train the network, there is not a clear multivariate function that could have been used for

---

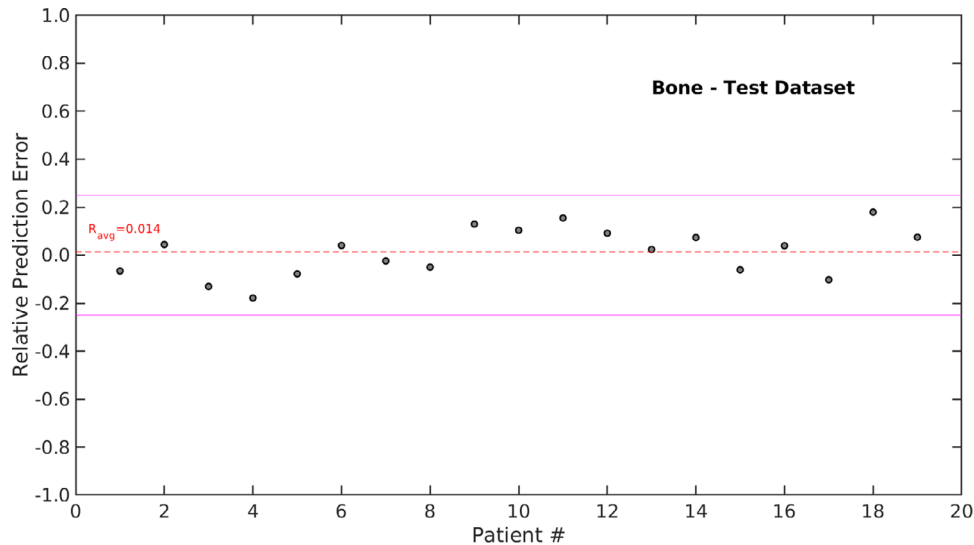[*] GE Revolution GSI 64 Technical Manual 5507106-1EN Rev 1, Ch. 16, pp. 17

FIGURE 8 Relative prediction error between deep learning predicted and Monte Carlo estimated bone dose values in the test dataset. The magenta lines indicate the 25% relative error limit. The red dashed line is the average error (R_{avg} = 1.4%).
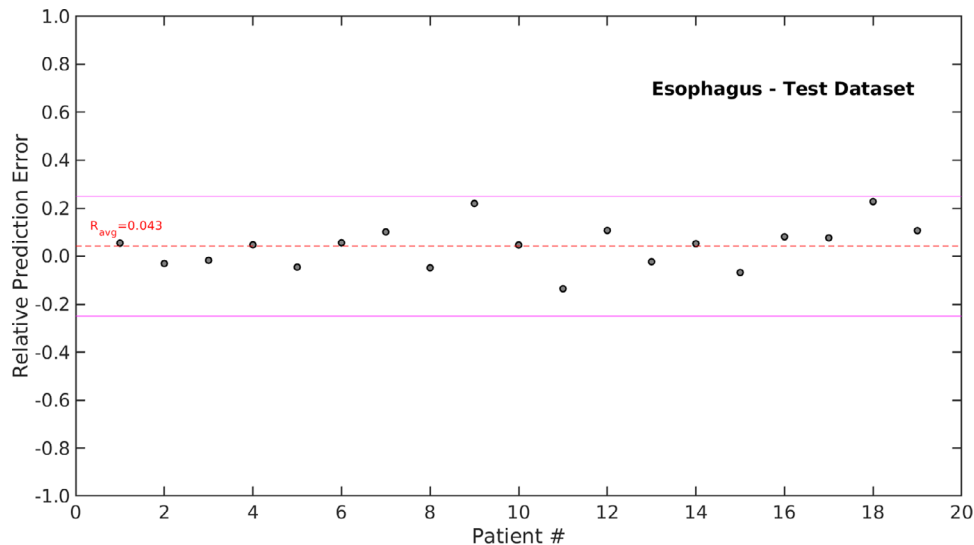

FIGURE 9 Relative prediction error between deep learning predicted and Monte Carlo estimated esophagus dose values in the test dataset. The magenta lines indicate the 25% relative error limit. The red dashed line is the average error (R_{avg} = 4.3%).

multivariate regression rather than a deep learning network model. In fact, it may be impossible to find a globally optimal function to fit every dose point of the data space.

The potential advantage of the direct organ-dose estimation method is that the training of the deep learning algorithm is considerably simplified and the required data set to achieve reasonable results can be constructed by a limited number of patients compared to methods that generate and segment images. Moreover, artificially generated dose images can be prone to artifacts that would not always be accounted for or corrected when the organ-dose calculation step is performed. Such artifacts are completely avoided with the method presented here. In addition, the deep learn-

ing algorithm itself is simple and easy to implement with any programming language and is not limited to MATLAB.

A further advantage of the method is the direct estimation of organ dose values for a specific patient based on input data that are readily available on the DICOM header of the CT images and can be applied during or immediately after patient imaging. The direct estimation of organ dose implies that the deep learning algorithm does not generate two- or three- dimensional dose images that would have required the application of a segmentation method to delineate the organ in question and then extract the relevant dose. Skipping the generation and segmentation of images, two computation
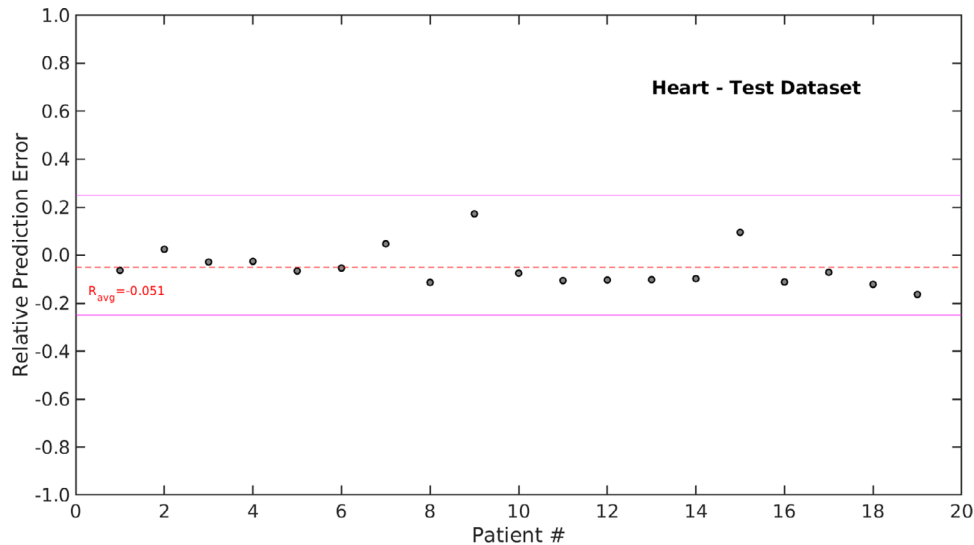
FIGURE 10 Relative prediction error between deep learning predicted and Monte Carlo estimated heart dose values in the test dataset. The magenta lines indicate the 25% relative error limit. The red dashed line is the average error ($R_{avg} = -5.1\%$).
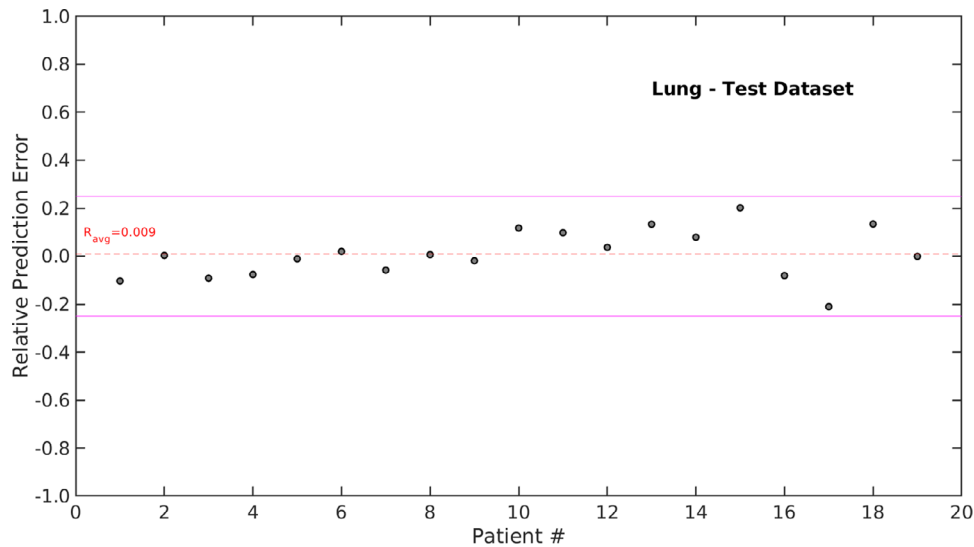

FIGURE 11 Relative prediction error between deep learning predicted and Monte Carlo estimated lung dose values in the test dataset. The magenta lines indicate the 25% relative error limit. The red dashed line is the average error ($R_{avg} = 0.9\%$).

steps are avoided that would have increased the final uncertainty in the calculated dose and the complexity of the deep learning algorithm. A potential workflow in a clinical setting would include the following steps without user interaction: a) the patient CT scan is acquired; b) the WED values are automatically calculated from patient images; c) scan length and tube-current are extracted from DICOM header; d) WED, scan length and tube current values inserted in the deep learning network and organ dose values predicted.

The proposed method is heavily influenced by the quality of the Monte Carlo dose values used for training. The uncertainty in the Monte Carlo estimated dose, for example, due to statistical limitations on x-ray photons or

HU conversion, will be propagated in the deep learning algorithm. However, by using dose over the contoured organ rather than pixel values of images as our training output, we avoid local uncertainties and extreme values, hence suppressing uncertainties on the final organ dose value.

Patients with contrast were excluded from this study. A different approach is required to generate Monte Carlo dose distributions for contrast-enhanced scans. This was deemed not necessary at this point since the current work was a proof-of-concept study for CT scans without contrast enhancement. Iodine uptake will change the local CT number, and this will be reflected on WED and mA. However, it is the CT number from

iodine particles concentration that changes rather than the local tissue. Before performing deep learning training, the Monte Carlo tool needs to properly consider contrast media particle distributions within tissues and associated differences in pharmacokinetics within different patients.[17] This is a non-trivial and computationally intensive simulation to perform and does not guarantee generality.

Future plans regarding the demonstrated methodology include the deployment in our clinic for a retrospective estimation of patient organ dose from thorax CT examinations and further validation of the deep learning model. Potential challenges regarding different CT scanners and iodine concertation have already been discussed in previous paragraphs. As in any deep learning algorithm, the training dataset essentially determines the quality of the predictions. Patients with underlying diseases that may have non-trivial effects on x-ray attenuation within tissues, and subsequently WED and mA modulation, may need to be separately treated if there are many such cases. In this work the data sample is representative of the patient population undergoing thorax CT examinations in our clinic. This is not applied to any clinic and may not even apply to a different CT scanner in the same clinic (e.g., dedicated to a specific group of patients), hence a new dataset for training may be required. Moreover, data for underrepresented population, such as obese and/or younger patients (Figure 2) may need to be added to the training set to improve prediction outcomes for those cases.

5 | CONCLUSION

Deep learning networks can be applied to obtain patient organ dose estimation for diagnostic CT imaging procedures nearly real-time. We proposed a method to rapidly estimate organ-dose for patients undergoing thoracic CT examinations that relies on a deep learning network with simple implementation and training.

CONFLICT OF INTEREST
Marios Myronakis is also affiliated with the Division of Medical Physics and Biophysics in Brigham and Women's Hospital (BWH), Dana Farber Cancer Institute (DFCI), Harvard Medical School (HMS). BWH, DFCI and HMS did not fund and were not involved with this project.

REFERENCES

1. Damilakis J, Dosimetry CT. *Invest Radiol*. 2021;56(1):62-68.
2. Kalender WA. Dose in x-ray computed tomography. *Phys Med Biol*. 2014;59(3):R129-R150.
3. McCollough CH, Bruesewitz MR, Kofler JM. CT dose reduction and dose management tools: overview of available options. *RadioGraphics*. 2006;26(2):503-512.
4. Lawson M, Berk K, Badawy M, Qi Y, Kuganesan A, Metcalfe P. Comparison of organ and effective dose estimations from different Monte Carlo simulation-based software methods in infant CT and comparison with direct phantom measurements. *J Appl Clin Med Phys*. 2022;23(6).
5. Chen W, Kolditz D, Beister M, Bohle R, Kalender WA. Fast on-site Monte Carlo tool for dose calculations in CT applications. *Med Phys*. 2012;39(6Part1):2985-2996.
6. Perisinakis K, Tzedakis A, Damilakis J. On the use of Monte Carlo-derived dosimetric data in the estimation of patient dose from CT examinations. *Med Phys*. 2008;35(5):2018-2028.
7. DeMarco JJ, Cagnon CH, Cody DD, et al. A Monte Carlo based method to estimate radiation dose from multidetector CT (MDCT): cylindrical and anthropomorphic phantoms. *Phys Med Biol*. 2005;50(17):3989-4004.
8. Maier J, Klein L, Eulig E, Sawall S, Kachelrieß M. Real-time estimation of patient-specific dose distributions for medical CT using the deep dose estimation. *Med Phys*. 2022;49(4):2259-2269.
9. Tzanis E, Damilakis J. A novel methodology to train and deploy a machine learning model for personalized dose assessment in head CT. *Eur Radiol*. 2022;32(9):6418-6426.
10. Götz TI, Schmidkonz C, Chen S, Al-Baddai S, Kuwert T, Lang EW. A deep learning approach to radiation dose estimation. *Phys Med Biol*. 2020;65(3):035007.
11. Schindelin J, Arganda-Carreras I, Frise E, et al. Fiji: an open-source platform for biological-image analysis. *Nat Methods*. 2012;9(7):676-682.
12. Picture thresholding using an iterative selection method. *IEEE Trans. Syst. Man. Cybern*. 1978;8(8):630-632.
13. McCollough C, Bakalyar DM, Bostani M, et al. Use of water equivalent diameter for calculating patient size and size-specific dose estimates (SSDE) in CT: the report of AAPM task group 220. *AAPM Rep*. 2014(220):6-23.
14. Deak P, van Straten M, Shrimpton PC, Zankl M, Kalender WA. Validation of a Monte Carlo tool for patient-specific dose simulations in multi-slice computed tomography. *Eur Radiol*. 2008;18(4):759-772.
15. Myronakis M, Perisinakis K, Tzedakis A, Gourtsoyianni S, Damilakis J. Evaluation of a patient-specific Monte Carlo software for CT dosimetry. *Radiat Prot Dosimetry*. 2009;133(4):248-255.
16. The Mathworks I. Deep Learning Toolbox: Natick, Massachusetts, United States. 2011. https://www.mathworks.com/help/deeplearning/
17. Sahbaee P, Abadi E, Segars WP, Marin D, Nelson RC, Samei E. The effect of contrast material on radiation dose at CT: part II. A systematic evaluation across 58 patient models. *Radiology*. 2017;283(3):749-757.